Proc. Natl. Acad. Sci. USA
Vol. 96, pp. 10495–10500, August 1999
Physiology

Disruption of myoglobin in mice induces multiple compensatory mechanisms

AXEL GÖDECKE*, ULRICH FLÖGEL*, KLAUS ZANGER†, ZHAOPING DING*, JENS HIRCHENHAIN‡, ULRICH K. M. DECKING*, AND JÜRGEN SCHRADER*‡§

*Institut für Herz und Kreislaufphysiologie, †Institut für Anatomie und Hirnforschung, and ‡Biologisch-Medizinisches Forschungszentrum, Heinrich-Heine-Universität Düsseldorf, Postfach 101007, 40001 Düsseldorf, Germany

Communicated by Ewald R. Weibel, University of Bern, Herrenschwanden, Switzerland, July 15, 1999 (received for review February 4, 1999)

ABSTRACT **Myoglobin may serve a variety of functions in muscular oxygen supply, such as O_2 storage, facilitated O_2 diffusion, and myoglobin-mediated oxidative phosphorylation. We studied the functional consequences of a myoglobin deficiency on cardiac function by producing myoglobin-knockout ($myo^{-/-}$) mice. To genetically inactivate the myoglobin gene, exon 2 encoding the heme binding site was deleted in embryonic stem cells via homologous recombination. $Myo^{-/-}$ mice are viable, fertile, and without any obvious signs of functional limitations. Hemoglobin concentrations were significantly elevated in $myo^{-/-}$ mice. Cardiac function and energetics were analyzed in isolated perfused hearts under resting conditions and during β-adrenergic stimulation with dobutamine. $Myo^{-/-}$ hearts showed no alteration in contractile parameters either under basal conditions or after maximal β-adrenergic stimulation (200 nM dobutamine). Tissue levels of ATP, phosphocreatine (^{31}P-NMR), and myocardial O_2 consumption were not altered. However, coronary flow {6.4 ± 1.3 ml·min^{-1}·g^{-1} [wild-type (WT)] vs. 8.5 ± 2.4 ml·min^{-1}·g^{-1} [$myo^{-/-}$]} and coronary reserve [17.1 ± 2.1 (WT) vs. 20.8 ± 1.1 ($myo^{-/-}$) ml·min^{-1}·g^{-1} were significantly elevated in $myo^{-/-}$ hearts. Histological examination revealed that capillary density also was increased in $myo^{-/-}$ hearts [3,111 ± 400 mm^{-2} (WT) vs. 4,140 ± 140 mm^{-2} ($Myo^{-/-}$)]. These data demonstrate that disruption of myoglobin results in the activation of multiple compensatory mechanisms that steepen the pO_2 gradient and reduce the diffusion path length for O_2 between capillary and the mitochondria; this suggests that myoglobin normally is important for the delivery of oxygen.**

Myoglobin is a small monomeric oxygen binding heme protein located in the cytosol of vertebrate muscles that are adapted to perform sustained work, such as cardiac myocytes and type I and IIa skeletal muscle (1). The half saturation of myoglobin with oxygen ($P_{50}O_2$) occurs at a PO_2 of 2.3 mmHg (1 mmHg = 133 Pa), which lies below the capillary PO_2 of 20–25 mmHg (1). Thus, myoglobin, at least under basal conditions, exists in a largely oxygenated state. In this form, it may serve as a short-term oxygen store during transitory hypoxia and may thus buffer oscillations of tissue PO_2 occurring, e.g., during systolic compression in the heart or during exercise in skeletal muscle (2). High concentrations of myoglobin exceeding those found in most terrestrial vertebrates by 5- to 10-fold are found in the muscles of diving vertebrates, suggesting that, in this case, myoglobin functions as a long-term O_2 store (3).

Myoglobin also has been proposed to facilitate oxygen diffusion from the sarcolemma to the mitochondria (3). The degree to which intracellular O_2 transport is enhanced by this process depends on the gradient of oxymyoglobin in the cytosol (1). According to this hypothesis, a flux of myoglobin-bound oxygen exists in parallel to the flux of dissolved oxygen. Facilitation of O_2 diffusion has been demonstrated unambiguously in concentrated myoglobin solutions (4). However, experiments designed to investigate this function of myoglobin in isolated cells or tissues yielded results that were less clear (5–10). In support of a functional role for facilitated O_2 diffusion, O_2 desaturation of myoglobin could be demonstrated by spectroscopic analysis of isolated cardiac myocytes or hearts (5–7). Moreover, chemical inactivation of myoglobin resulted in reduced cardiac performance (8). However, a recent NMR study in the dog heart *in situ* found no measurable myoglobin deoxygenation under resting conditions (9). Likewise, chemical inactivation of myoglobin in cardiac myocytes or isolated canine hearts by means of nitrite or H_2O_2 application did not reveal a significant contribution of myoglobin to O_2 transport (10, 11). Model calculations also yield conflicting results that have both supported and refuted a contribution of myoglobin-bound oxygen to total oxygen flux (12, 13). In sum, the extent to which myoglobin is involved in facilitated O_2 diffusion is still a matter of debate.

All previous experiments aimed at elucidating the functional role of myoglobin were performed by using chemical inactivation such as CO, nitrite, or hydrogen peroxide (8, 11, 14). Interpretation of the data is based on the assumption that the chosen inhibitors are selective and do not critically perturb other cellular functions. However, recent experimental data demonstrated, at least for nitrite, nonspecific side effects (15). In this situation, gene targeting techniques offer an important alternative to study loss of function of a gene product because they allow the selective removal of specific genes. In a recent publication, this approach was applied to disrupt synthesis of myoglobin genetically (16). It was found that a loss of myoglobin did not alter the exercise capacities of mice, leading to the conclusion that myoglobin is not essential for normal cardiac and skeletal muscle function (16). In independently generated myoglobin knockout mice presented in this study, we have analyzed cardiac structure and function in greater detail. We have found that chronic loss of myoglobin results in the activation of compensatory mechanisms that all tend to steepen the PO_2 gradient to the mitochondria. Compensatory mechanisms include a higher capillary density, increase in coronary flow and coronary flow reserve, and elevated hematocrit. These facts all suggest that myoglobin is likely to be important for normal cardiac function and that it may serve a critical role in the delivery of oxygen to the mitochondria.

MATERIALS AND METHODS

Generation of $Myo^{-/-}$ mice. Myoglobin-specific genomic clones were isolated from a genomic library of mouse strain 129Sv by using a 266-bp, PCR-amplified cDNA fragment of the

The publication costs of this article were defrayed in part by page charge payment. This article must therefore be hereby marked "*advertisement*" in accordance with 18 U.S.C. §1734 solely to indicate this fact.

PNAS is available online at www.pnas.org.

Abbreviations: PCr, phosphocreatine; kb, kilobase; WT, wild-type; V-PO_2, coronary venous PO_2.

§To whom reprint requests should be addressed. E-mail: schrader@uni-duesseldorf.de.

murine myoglobin gene spanning exon 2. The targeting vector was constructed by replacing a 1.2-kb *Xba*I/*Hin*dIII fragment spanning exon 2 that encodes the essential heme binding site by the neomycin resistance (*neo*^{R}) gene (Fig. 1*a*). This was achieved by inserting a 0.9-kb *Hin*cII-*Xba*I fragment 5′ and an 8-kb *Hin*dIII fragment 3′of the neo^R gene. The embryonic stem cell line R1 (17) was transfected with the linearized targeting construct, and cultivation and selection of transfected clones was carried out as described (18). Correctly targeted clones were identified via PCR by using the following primers: Myo, 5′-GAGGGAGCTGGTGTCAACAG-3′; neo, 5′-CTTGCAAAACCACACTGCTC-3′. Three of ninety-eight clones screened were correctly targeted, and two of these were used for generation of chimeric mice. Embryonic stem cells were aggregated with day-2.5 murine embryos isolated from strain NMRI according to published procedures (19). Chimeric males were crossed with NMRI females, and the agouti-colored offspring were analyzed for transmission of the myoglobin mutation. Heterozygous animals were intercrossed to generate homozygously mutated animals. Wild-type (WT) siblings obtained from the offspring of these crosses were used as control animals in the experiments.

For Southern blot analysis of different genotypes, 10 μg of *Bgl*II-digested mouse tail DNA were hybridized with a 1.4-kb *Hin*dIII-*Bam*HI-fragment as indicated in Fig. 1*a*. For Northern blot analysis, 5 μg of total RNA were separated on 1.2% formaldehyde gels, were transferred to HybondN membranes (Amersham Pharmacia), and were hybridized by using the 0.26-kb myoglobin cDNA fragment described above. For SDS/PAGE analysis, 200 μg of protein extracts from blood free hearts were loaded on a 12.5% gel that was stained with Coomassie brilliant blue according to standard procedures.

Measurements of myoglobin concentrations in WT mouse hearts were performed by densitometric scanning of cardiac protein extracts separated by SDS/PAGE. Myoglobin-specific bands were quantified by standardization with known amounts of horse myoglobin (Sigma).

Heart Perfusion and ^{31}P-NMR Spectroscopy. Preparation of murine hearts, retrograde perfusion, and ^{31}P-NMR spectroscopy were performed essentially as described (20). Total body weight ranged from 25–35 g, and heart weight from 180 to 230 mg. No significant differences between both groups were observed. Also, the heart/body weight ratios were identical between WT and myo$^{-/-}$ mice. For determination of coronary venous PO_2 (V-PO_2) the pulmonary artery was cannulated, and V-PO_2 was measured with a Clark type oxygen electrode. Arterial PO_2 was ≈680 mmHg. Oxygen consumption was calculated according to Fick's principle as the product of the arterio-venous O_2 content difference and coronary flow. Data were normalized for heart weights. To determine basal cardiac ATP, creatine, and PCr levels, mice hearts of each strain were snap-frozen in a separate series of experiments (n = 8 in each group) under baseline conditions. Hearts were subsequently extracted with 1 M perchloric acid as described

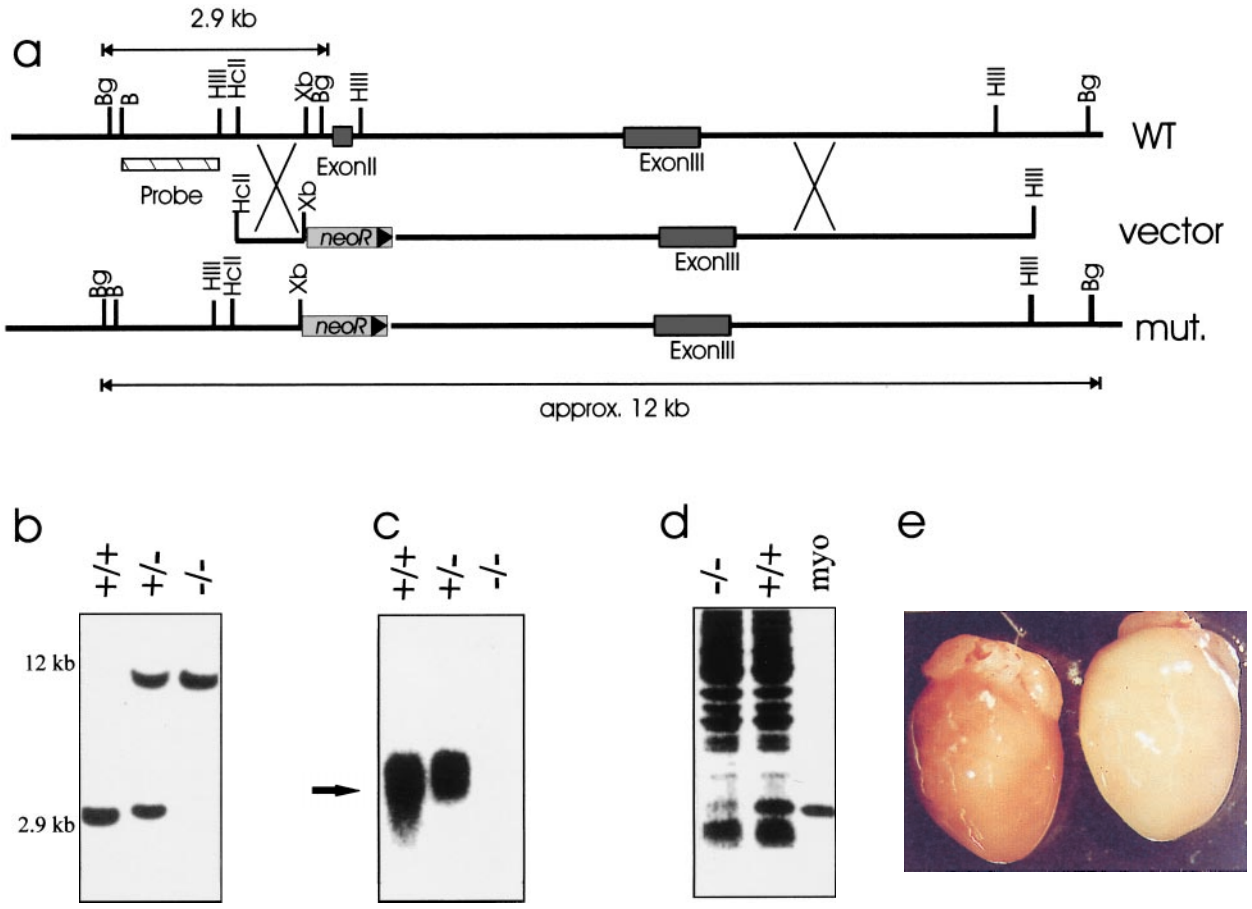

FIG. 1. Targeting strategy and molecular verification of myoglobin disruption. (*a*) Structures of the WT and mutated alleles (mut) and the targeting vector are shown. (Restriction sites: B, *Bam*HI; Bg, *Bgl*II; HIII, *Hin*dIII; HcII, *Hin*cII; Xb, *Xba*I. *neoR*, neomycin resistance gene). (*b*) Southern blot analysis of *Bgl*II-digested DNA from WT (+/+), heterozygous (+/−), and homozygously mutated (−/−) mice. The *Bam*HI-*Hin*dII-fragment indicated in *a* was used as a probe. Hybridizing fragments of 2.9 kb (WT allele) and 12 kb (mutated allele) were detected. (*c*) Northern blot analysis of cardiac RNA isolated from the three genotypes. (*d*) SDS/PAGE analysis of protein patterns of myo$^{-/-}$ and WT hearts. Two-hundred micrograms of cardiac proteins were separated on a 12.5% SDS gel and were stained with Coomassie brilliant blue. Five micrograms of horse myoglobin were loaded as control. (*e*) Morphology of myoglobin-deficient hearts. WT (left) and myo$^{-/-}$ hearts (right) were perfused free of blood and were photographed.

(20). Baseline spectra of each series were related to the respective HPLC data, assuming 100% NMR visibility for ATP. Peak areas obtained by integration were converted to concentrations on the basis of a cytosolic water space of 4.3 μl/mg protein, which was calculated as described (20). PCr concentrations were determined from the PCr/ATP ratio measured by NMR. Peak areas were scaled according to saturation factors of the respective phosphorous compounds determined from fully relaxed ^{31}P NMR spectra (flip angle 90°, repetition time 15 s) in control experiments for each strain (wild-type, PCr = 0.371 ± 0.023, ATP = 0.697 ± 0.045; myo$^{-/-}$, PCr = 0.376 ± 0.020, ATP = 0.634 ± 0.046; n = 8 for each group). After equilibration of the hearts within the magnet, ^{31}P NMR spectra were continuously recorded with a temporal resolution of 4 min.

Morphometric Procedures. For morphometric analyses, cardiac tissue was prepared as follows: Mice were killed by cervical dislocation, the thorax was opened rapidly, and a 23-gauge cannula was inserted into the ascending aorta. Hearts were perfused in a retrograde direction with Krebs–Henseleit buffer for 5 min followed by 5 min of perfusion with fixative (2.5% glutaraldehyde in 0.1 M cacodylate buffer). Perfusion pressure was 100 mm Hg. Hearts were excised and postfixed overnight in the same fixative. A total of 24 myocardial tissue samples were obtained from six WT and six myo$^{-/-}$ hearts from the free wall of the left ventricle by using the left descending coronary artery as a landmark.

For electron microscopical investigation, fixed tissue samples were rinsed twice in cacodylate buffer (0, 1 M) for 10 min and were postfixed in 2% osmium tetroxide in the same buffer for 2 h at room-temperature. After washing twice for 10 min in the same buffer, specimens were dehydrated in a graded acetone series (70% acetone containing 1% phosphotungsten acid and 0,5% uranyl acetate for block contrasting). Tissues were embedded in SPURR (Serva). Ultra-thin sections (Ultramicrotome Om-U2, Reichert) were cut from the embedded tissues and were mounted and stained for 30 min by floating the grids on drops of uranyl acetate. Sections were viewed in an H 600 electron microscope (Hitachi, Tokyo).

A total of 137 digital micrographs of different areas of the specimen grids were used with an original magnification of 2,500-fold. Ten to twelve micrographs per sample were analyzed for mitochondrial density by using the point-counting method with a grid with effective line separation of 1.5 μm superimposed digitally on the pictures.

For measurements of capillary densities, semi-thin sections were carried out from the embedded tissues as well. Sections were stained with 5% toluidin-blue and were examined with an Olympus (New Hyde Park, NY) microscope combined with a computerized digital analysis system (Soft Imaging Systems, Münster, Germany). Micrographs were overlayed with a grid (50 μm square), and the numbers of capillaries per 10 squares were counted. Capillary distances were determined independently by measuring the distances between capillaries in micrographs by connecting capillary centers on screen using the distance measurement function of the soft imaging system digital image analysis system. A total of 600 capillary distances for each group (100 per animal) were analyzed.

Blood Parameters. For the analysis of hematocrit and hemoglobin concentration, blood was collected by cardiac puncture from ether-anesthetized mice and was mixed with 5 μl of 0.5 M EDTA. Hematocrit was determined by centrifugation of blood in sealed heparinized capillaries. Hemoglobin concentrations were calculated from the absorbance of cyanmethemoglobin at 546 nm.

Statistical Analysis. Data were analyzed by two-tailed, two-sided Student's t test. Repeated measurements (Fig. 3) were analyzed by using two way ANOVA (SPSS 8.0, SPSS, Chicago). Differences were assumed to be significant with a P value <0.05.

RESULTS

Analysis of the genomic structures of mice of all three myoglobin genotypes of the F2-offspring revealed that the myoglobin locus was properly targeted (Fig. 1*b*). Northern blot analysis of total cardiac RNA demonstrated the absence of myoglobin specific RNA in Myo$^{-/-}$ mice (Fig. 1*c*). Accordingly, in cardiac protein extracts, no myoglobin was detectable (Fig. 1*d*). Myoglobin-deficient mice were viable, fertile, and without any sign of functional limitations.

Isolated perfused hearts from myo$^{-/-}$ mice showed a yellow color in contrast to the pale red appearance of the WT hearts (Fig. 1*e*). Measurements of myoglobin concentrations in WT mouse hearts were performed by densitometric scanning of cardiac protein extracts separated by SDS/PAGE. Cardiac myoglobin content was determined to be 0.19 ± 0.3 mmol of myoglobin/kg wet weight (n = 4).

In further experiments, hematocrits and hemoglobin concentrations were studied in WT and myo$^{-/-}$ mice. Hemoglobin concentrations were slightly but significantly elevated in myo$^{-/-}$ mice (Table 1). The hematocrit was also higher in myo$^{-/-}$ mice, but this difference did not reach the level of significance. Because the hemoglobin concentrations in erythrocytes (hemoglobin:hematocrit ratio) were identical in both groups, the oxygen transport capacity was elevated most likely by an augmented hematocrit.

To assess the effect of the myo$^{-/-}$ mutation on cardiac performance, basal functional parameters were measured in isolated perfused hearts from WT and Myo$^{-/-}$ mice. As shown in Fig. 2, contractile parameters such as left ventricular pressure and dP/dt_{max} (rate of maximal pressure development) were not altered. Similarly, dP/dt_{min} was not different (data not shown). In line with this finding, oxygen consumption (MVO_2) was not significantly different between WT and myo$^{-/-}$ hearts. Coronary V-PO_2 tended to be higher in myo$^{-/-}$ hearts, but the differences did not reach statistical significance. However, basal coronary flow was significantly elevated by ≈30% in myo$^{-/-}$ mice. Simultaneously with the assessment of cardiac function, metabolic parameters reflecting cardiac energetics such as ATP and PCr were determined by ^{31}P-NMR. No differences in ATP and PCr concentrations or the ATP/PCr ratio were detected (Fig. 2).

To explore whether cardiac performance of hearts from myo$^{-/-}$ mice were compromised when stressed, experiments were carried out with dobutamine (50, 200 nM). As shown in Fig. 3, stimulation of WT hearts with dobutamine resulted in a dose-dependent increase of left ventricular pressure by 83% (50 nM) and 100% (200 nM). In myo$^{-/-}$, the dobutamine-stimulated increase in left ventricular pressure tended to be higher as compared with WT hearts, but the differences did not reach significance. Similarly, no differences in dP/dt_{max} were evident (data not shown). In WT hearts, oxygen consumption increased from basal levels of 6.0 ± 1.1 μmol·min^{-1}·g^{-1} by 66 and 83% at 50 at 200 nM dobutamine, respectively. In myo$^{-/-}$ hearts, an almost identical increase of MVO_2 was measured. In contrast, the dobutamine-induced increase in coronary flow was significantly higher in myo$^{-/-}$ hearts. This difference was +33% under basal conditions (P = 0.06, n = 8) and +25% under stimulation with 50 and 200 nM dobutamine ($P < 0.05$, n = 8). Significant differences also were

Table 1. Hematocrit and hemoglobin concentration in myoglobin-deficient mice

	WT	Myo$^{-/-}$	
Hb, g/dl	13.3 ± 0.6	14.4 ± 0.5	P = 0.02
Hct, vol. %	49.1 ± 3.3	52.5 ± 4.3	n.s.
Hb/Hct	0.27	0.27	

Values are given as means ± SD of n = 8 (WT) and n = 9 (myo$^{-/-}$) mice. n.s., not significant; Hb, hemoglobin; Hct, hematocrite.

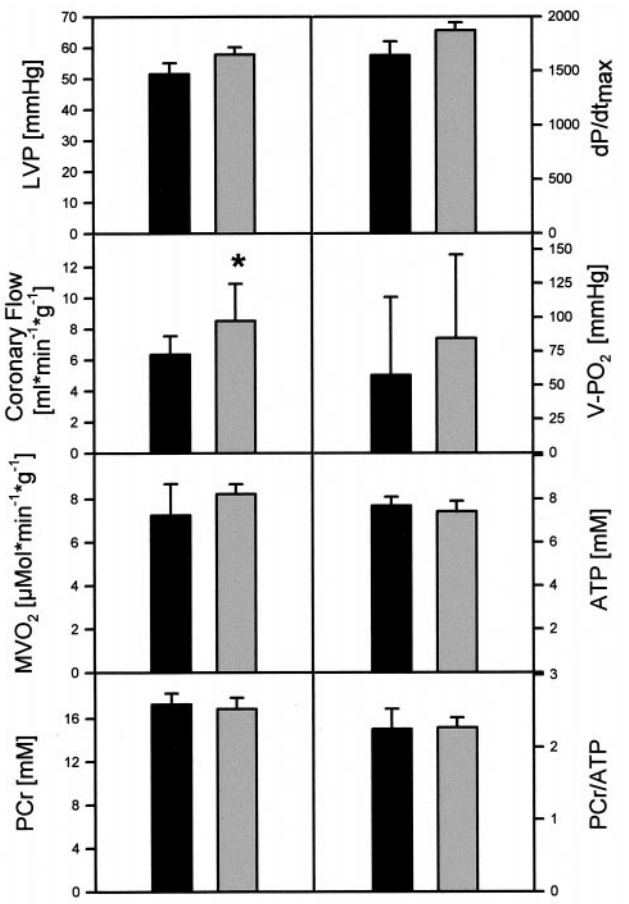

FIG. 2. Analysis of cardiac function and energetics of isolated perfused WT and myo$^{-/-}$ hearts under basal conditions. Bars show the means ± SD for $n = 8$ hearts from WT (black bars) and myo$^{-/-}$ hearts (gray bars). *, statistically significant ($P < 0.05$). LVP, left ventricular pressure; dP/dt_{max}, rate of maximal pressure development; MVO_2, oxygen consumption.

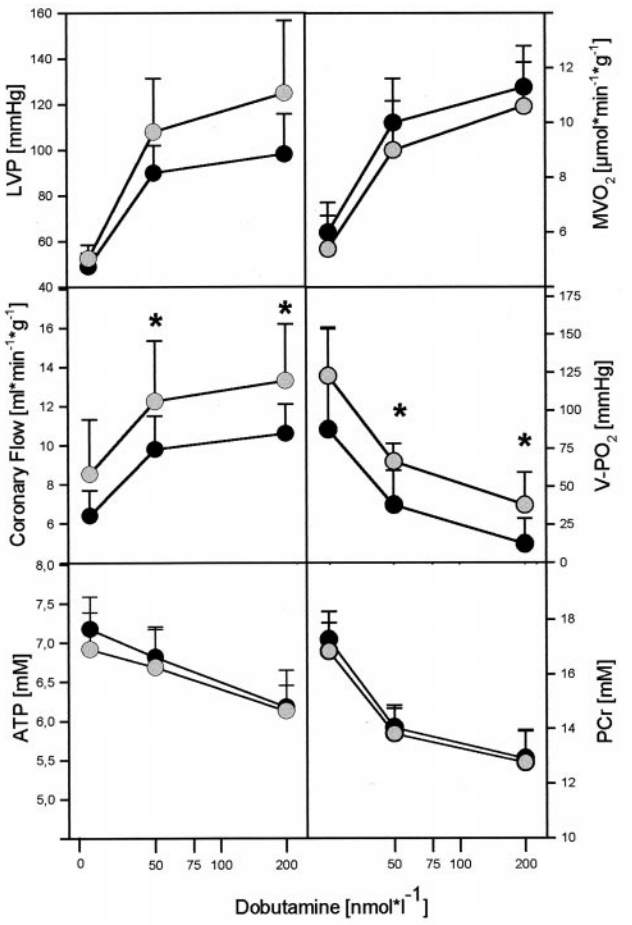

FIG. 3. Analysis of cardiac function and energetics of isolated perfused WT and myo$^{-/-}$ hearts under β-adrenergic stimulation. Hearts were stimulated by coronary application of 50 or 200 nM dobutamine. Symbols show means ± SD for $n = 8$ hearts from WT (black) and myo$^{-/-}$ hearts (open symbols). *, statistically significant ($P < 0.05$). For abbreviations see Fig. 2.

found for coronary $V\text{-}PO_2$. $V\text{-}PO_2$ decreased in WT from a basal value of 88 mmHg to 38 and 12.5 mmHg at 50 and 200 nM dobutamine, respectively. In myo$^{-/-}$ hearts, $V\text{-}PO_2$ was always higher as compared with WT hearts. Under basal conditions, $V\text{-}PO_2$ was 123 mmHg and fell to 67 and 38 mmHg at 50 and 200 nM dobutamine, respectively.

^{31}P-NMR analysis of cardiac energetics revealed that ATP and PCr decreased with increasing β-adrenergic stimulation. In WT hearts, the intracellular ATP concentrations amounted to 7.7 ± 0.4 mM under control conditions and decreased by 4.8 and 13.1% at 50 and 200 nM dobutamine, respectively. In myo$^{-/-}$ hearts, the absolute ATP concentration as well as the ATP decline were not different. Also, the absolute PCr concentrations and the relative PCr-decline with increasing β-adrenergic stimulation were not different in both genotypes.

Because myo$^{-/-}$ hearts displayed a higher basal coronary flow, we tested whether coronary reserve was altered. Maximal coronary flow was elicited by intracoronary infusion of adenosine (1 μM) or as peak flow of reactive hyperemia after 20 s of coronary occlusion. As shown in Fig. 4, the maximal coronary flow response was significantly elevated in myo$^{-/-}$ hearts by ≈25%.

Myoglobin mutation resulted in important structural alterations. Data summarized in Fig. 5 show that capillary density was increased from 3,111 ± 400 mm^{-2} in the WT to 4,140 ± 140 mm^{-2} in myo$^{-/-}$ hearts. This resulted in a significant decline in mean capillary distance by 2.5 μm in myo$^{-/-}$ hearts.

To determine whether a redistribution of mitochondria occurred in addition to the changes in capillary density, a detailed morphometric analysis was performed. As summarized in Table 2, mitochondrial density was not different between WT and myo$^{-/-}$ hearts. In addition, the mitochondrial density in the perivascular area, defined as an area falling into a region of 5 μm from the capillary wall, also was not altered. In line with these morphometric findings, total cardiac cytochrome *c* oxidase activity was the same in both groups (Table 2).

DISCUSSION

This study reports that targeted disruption of myoglobin in mice leaves cardiac function uncompromised. Normal function was most likely the result of activation of multiple compensatory mechanisms that collectively can substitute for the loss of myoglobin function in the heart. Functional adaptations include elevation of basal coronary flow, coronary flow reserve, capillary density, and hematocrit. All of these factors tend to steepen the PO_2 gradient from the capillary to the mitochondria, which is in support of the view that myoglobin plays a critical role in the delivery of oxygen in vertebrates.

The knockout strategy to generate myoglobin-deficient mice aimed to delete exon 2 of the myoglobin gene because, due to the sequence of the murine myoglobin gene, this exon encodes the major part of myoglobin, including essential sequence

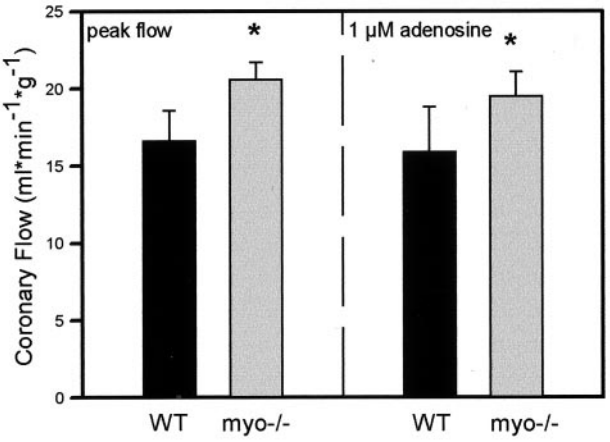

FIG. 4. Coronary flow reserve in WT and myo$^{-/-}$ hearts. Maximal coronary flow of WT and myo$^{-/-}$hearts was determined as peak flow of reactive hyperemia elicited by 20 s of coronary occlusion or as maximal vasodilation in response to intracoronary application of 1 μM adenosine. Bars show means ± SD for $n = 6$ WT (black bars) and myo$^{-/-}$ hearts (gray bars). *, statistically significant ($P < 0.05$).

elements involved in heme binding (21). Several lines of evidence demonstrate a successful inactivation of the myoglobin locus: (*i*) Southern blot analysis revealed the characteristic changes in the genomic structure of the myoglobin locus expected for a correct targeting event. (*ii*) RNA isolated from myo$^{-/-}$ but not WT or myo$^{+/-}$ hearts was devoid of a myoglobin-specific signal in Northern blot analysis. (*iii*) Because myoglobin belongs to the highly expressed cardiac proteins, myoglobin deficiency could be detected even by SDS/PAGE. (*iv*) The color of cardiac muscle shifted from a pale red in WT to yellow in myo$^{-/-}$ hearts.

Similar to a recent report by Garry *et al.* (16), we found that mice without myoglobin generated by gene knockout technology are fertile and show no obvious phenotypic abnormalities during ambient activities. These authors suggested that more extreme physiological challenges might reveal abnormalities between WT and knockout mice. In the present study, we have challenged isolated perfused hearts from myo$^{-/-}$ mice with maximal β-adrenergic stimulation and found no difference in

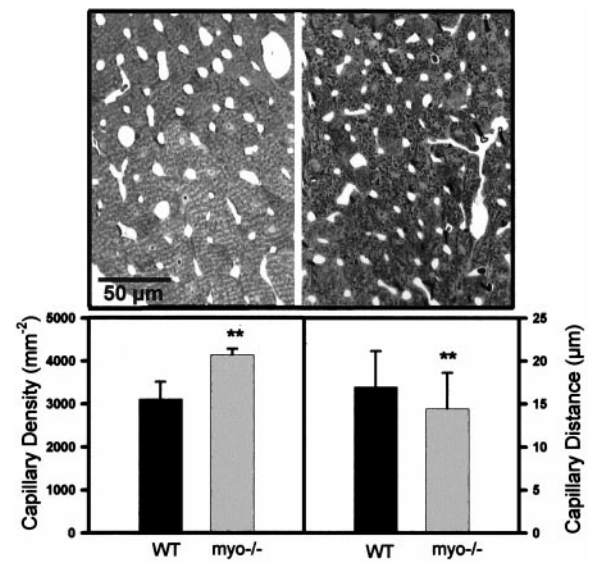

FIG. 5. Analysis of capillary densities in WT and myo$^{-/-}$ hearts. Representative micrographs for WT (left) and myo$^{-/-}$ hearts (right) are shown together with the quantitative data for capillary density and capillary distance. Bars represent means ± SD for 6 WT (black bars) and 6 myo$^{-/-}$ hearts (gray bars). **, statistically significant ($P < 0.01$).

left ventricular performance when compared with WT hearts. Because all hearts were paced at the same frequency, it follows that the rate-pressure product, a sensitive index of cardiac work, remained unchanged. In line with this finding, basal and stimulated O_2 consumption was not different between WT and myo$^{-/-}$ hearts.

In addition to mechanical parameters, we assessed cardiac energetics by measuring, with ^{31}P-NMR, changes in the concentration of ATP and PCr. Both metabolites are known to be tightly coupled with oxidative phosphorylation and, thus, may represent a sensitive index of cardiac oxygen supply. NMR data revealed that ATP and PCr levels were the same in the unstressed hearts of WT and myo$^{-/-}$ mice. More importantly, the decline in ATP and PCr observed after β-adrenergic stimulation with dobutamine in WT hearts was indistinguishable from that found in myo$^{-/-}$ hearts. Thus, loss of myoglobin is not associated with compromised cardiac energetics. These data seem to suggest *prima facie* that myoglobin is not required to meet the metabolic requirements of the normal and of the stressed heart (16).

This study, however, uncovered important functional and structural differences between WT and myo$^{-/-}$ hearts. Coronary flow was significantly higher in unstressed myo$^{-/-}$ hearts. In dobutamine-stimulated hearts, this difference remained, in that coronary flow increased in parallel to the WT controls, reaching significantly higher maximal flow levels. In line with this finding is the observation that pharmacologically induced coronary flow reserve was significantly higher in myo$^{-/-}$ hearts as compared with WT controls. These functional differences are mirrored by differences in morphology. Capillary density in myo$^{-/-}$ hearts was increased by 30%, from 3,111 to 4,140 mm^{-2}, thereby significantly reducing capillary distance.

A further compensatory mechanism might involve an increase in mitochondrial density or a relocation of mitochondria into the vicinity of the capillaries. This would place mitochondria into a region of higher PO_2 and thereby would shorten the required diffusion distance for O_2. Morphometric analysis and measurements of cytochrome *c* oxidase demonstrated that neither the total mitochondrial density nor the mitochondrial fraction in the vicinity of the capillaries was elevated in myo$^{-/-}$ hearts.

PO_2 gradients from the capillary bed to the mitochondria are the major driving forces for tissue oxygenation. Significant extracellular PO_2 gradients from capillary blood to the sarcolemma have been reported as measured by spectrophotometric techniques (1, 5) and ^{1}H NMR (22). In contrast, the intracellular PO_2 profiles are remarkably shallow under resting conditions as well as with enhanced respiration (5, 23). More recently, these intracellular O_2 gradients were directly visualized with a radial spatial resolution of 4 μm in single cardiomyocytes (7). These radial PO_2 profiles appear to be critical for oxidative phosphorylation at increased oxygen demand but are also conceptually important for invoking a need for myoglobin-facilitated diffusion of oxygen (1). In myo$^{-/-}$ mice, there are at least three parameters changed, all of which tend to steepen the oxygen gradient from the capillary to the mito-

Table 2. Effects of the myoglobin mutation on mitochondrial density and distribution

	WT	myo$^{-/-}$	
Mitochondrial density, vol %	34 ± 2.6	31 ± 4.2	n.s.
Perivascular mitochondrial density,* vol %	32.8 ± 1.9	33.2 ± 2.8	n.s.
cytochrome *c* oxidase, μmol·min^{-1}·g^{-1}	86.6 ± 12.3	88.4 ± 19.4	n.s.

$n = 6$ in each group; means ± SD. n.s., not significant.
*The perivascular mitochondrial density was determined in the area of 5 μm around capillaries.

chondria and thereby augment the flux of oxygen: (*i*) Coronary flow is significantly increased under control conditions and in the stressed heart. This provides more oxygen per unit of time. Because MVO_2 was found unchanged in myo$^{-/-}$ hearts, this consequently resulted in an increased coronary venous PO_2 in our experimental model. (*ii*) Capillary density is increased in myo$^{-/-}$ hearts, so that the diffusion distance from each capillary to the core of the myocyte is significantly reduced. (*iii*) The oxygen carrying capacity in blood of myo$^{-/-}$ mice is significantly elevated, which can be expected to attenuate the longitudinal oxygen gradient along each capillary.

According to results by Hoppeler and Weibel (24), a key determinant of muscle oxygen supply is the concentration of erythrocytes around myocytes. Taking into account that capillary density was increased by 33% and hemoglobin concentration (hematocrit) by 8% in myoglobin-deficient hearts, erythrocyte concentration around cardiac myocytes may have been increased by 44%. Thus, the compensatory mechanisms appear to provide sufficient oxygen flux to the mitochondria to sustain cardiac hemodynamics and energetic parameters despite the lack of myoglobin.

In addition to its role in oxygen storage, myoglobin has been postulated to facilitate the diffusion of oxygen through the sarcoplasm (3). This hypothesis was recently challenged by Jürgens *et al.* (13) on the basis of new measurements of the diffusion coefficient of native myoglobin. On the other hand, there is functional evidence from Taylor *et al.* (8) that, after pharmacological abolition of the myoglobin O_2 binding function in the heart, there is a reduction in the maintenance of cardiac high energy phosphates under hypoxic conditions.

For myoglobin-facilitated oxygen diffusion to take place, myoglobin must be partially desaturated with oxygen. Using cryospectroscopy, Gajesky and Honig (6) found 50% of myocardial myoglobin normally to be in the deoxygenated state. More recently, Chen *et al.* (9) used ^{1}H-NMR spectroscopy to detect deoxymyoglobin in the blood-perfused beating heart. They found that, with unrestricted coronary flow, almost all of the myoglobin was oxygenated and that a linear relationship exists between the fractional desaturation of myoglobin and reduction of coronary flow at normal workload. These data do not exclude the possibility that unrestrained animals normally go through cycles of rest and physical activity, which is likely to be associated with fluctuations in the ratio of deoxy- to oxymyoglobin as well.

In addition to facilitated diffusion, myoglobin was postulated by Gupta and Wittenberg (14) to directly mediate oxygen delivery to mitochondria by an as yet unknown mechanism. According to this model, myoglobin-bound oxygen augments oxidative phosphorylation under conditions of excess oxygen supply when the respiratory chain is fully saturated by dissolved oxygen (4, 14, 25, 26). Supportive evidence was recently provided by Glabe *et al.* (15), who titrated the inactivation of myoglobin with CO by using ^{1}H-NMR. This hypothesis, however, is unlikely to explain our findings because myo$^{-/-}$ hearts displayed an unchanged myocardial oxygen consumption under conditions of elevated oxygen supply.

In summary, we have shown that chronic loss of myoglobin is associated with the induction of multiple mechanisms that steepen the longitudinal and radial gradient for oxygen in the heart. These compensatory mechanisms appear to explain the fact that cardiac function and energetics are uncompromised in myo$^{-/-}$ mice. They also strongly suggest that myoglobin normally fulfills an important function in the delivery of oxygen to the heart, most likely by myoglobin-facilitated diffusion.

We thank S. Küsters and B. Patzer for excellent technical assistance. We also thank Professor Duling (Univ. of Virginia, Charlottesville) for reading the manuscript. This work was supported by a grant from the Biologisch-Medizinisches Forschungszentrum der Heinrich-Heine-Universität Düsseldorf.

1. Wittenberg, B. A. & Wittenberg, J. B. (1989) *Annu. Rev. Physiol.* **51**, 857–878.
2. Millikan, G. A. (1937) *Proc. R. Soc. London Ser. B* **123,** 218–241.
3. Wittenberg, J. B. (1970) *Physiol. Rev.* **50,** 559–636.
4. Wittenberg, J. B. (1959) *Biol. Bull.* **117,** 402.
5. Wittenberg B. A. & Wittenberg, J. B. (1985) *J. Biol. Chem.* **260,** 6548–6554.
6. Gajesky, T. E. J. & Honig, C. R. (1991) *Am. J. Physiol.* **260,** H522–H531.
7. Takahasi, E., Sato, K., Endoh, H., Xu, Z. & Doi, K. (1998) *Am. J. Physiol.* **275,** H225–H233.
8. Taylor, D. J., Matthews, P. M. & Radda, G. K. (1986) *Respir. Physiol.* **63,** 275–283.
9. Chen, W., Zhang, J., Eljgelshoven, M. H., Zhang, Y., Zhu, X. H., Wang, C., Cho, Y., Merkle, H. & Ugurbil, K. (1997) *Magn. Reson. Med.* **38,** 193–197.
10. Jones, D. P. & Kennedy, F. G. (1982) *Biochem. Biophys. Res. Commun.* **105,** 419–424.
11. Cole, R. P., Wittenberg, P. A. & Caldwell, P. R. (1978) *Am. J. Physiol.* **234,** H567–H572.
12. Groebe, K. (1995) *Biophys. J.* **68,** 1246–1269.
13. Jürgens, K. D., Peters, T. & Gros, G. (1994) *Proc. Natl. Acad. Sci. USA* **91,** 3829–3833.
14. Gupta, R. K. & Wittenberg, B. A. (1991) *Am. J. Physiol.* **261,** H1155–H1163.
15. Glabe, A., Chung, Y., Xu, D. & Jue, T (1998) *Am. J. Physiol.* **274,** H2143–H2151.
16. Garry, D. J., Ordway, G. A., Lorenz, J. N., Radford, N. B., Chin, E. R., Grange, R. W., Bassel-Duby, R. & Williams, R. S. (1998) *Nature (London)* **395,** 905–908.
17. Nagy, A., Rossant, J., Nagy, R., Abramov-Newerly, W. & Roder, J. C. (1993) *Proc. Natl. Acad. Sci. USA* **93,** 8424–8428.
18. Gödecke, A., Decking, U. K. M., Ding, Z., Hirchenhain, J., Bidmon, H.-J., Gödecke, S. & Schrader, J. (1998) *Circ. Res.* **82,** 186–194.
19. Wood, S. A., Pascoe, W. S., Schmidt, C., Kemler, R., Evans, M. J. & Allen, N. D. (1993) *Proc. Natl. Acad. Sci. USA* **90,** 4582–4585.
20. Flögel, U., Decking U. K. M., Gödecke, A. & Schrader J. (1999) *J. Mol. Cell. Cardiol.* **31,** 827–836.
21. Blanchetot, A., Price, M. & Jeffreys, A. J. (1986) *Eur. J. Biochem.* **159,** 469–474.
22. Kreutzer, U. & Jue, T. (1995) *Am. J. Physiol.* **268,** H1675–H1681.
23. Katz, I. R., Wittenberg, J. B. & Wittenberg, B. A. (1984) *J. Biol. Chem.* **259,** 7504–7509.
24. Hoppeler, H. & Weibel, E. R. (1998) *J. Exp. Biol.* **201,** 1051–1064.
25. Wittenberg B. A. & Wittenberg J. B. (1987) *Proc. Natl. Acad. Sci. USA* **84,** 7503–7507.
26. Doeller, J. E. & Wittenberg, B. A. (1991) *Am. J. Physiol.* **261,** 53–62.